Vol. 406: 57–70, 2010
doi: 10.3354/meps08571

MARINE ECOLOGY PROGRESS SERIES
Mar Ecol Prog Ser

Published May 10

PSII photoinhibition and photorepair in *Symbiodinium* (Pyrrhophyta) differs between thermally tolerant and sensitive phylotypes

Maria Ragni[1,*], Ruth L. Airs[2], Sebastian J. Hennige[1], David J. Suggett[1], Mark E. Warner[3], Richard J. Geider[1]

[1]Department of Biological Sciences, University of Essex, Colchester CO4 3SQ, UK
[2]Plymouth Marine Laboratory, Prospect Place, The Hoe, Plymouth PL1 3DH, UK
[3]University of Delaware, 700 Pilottown Rd., Lewes, Delaware 19958, USA

ABSTRACT: Cnidarians containing symbiotic microalgae often inhabit highly variable light environments where successful growth requires that, during transient (potentially stressful) periods of high light (HL), the microalgal cells invest energy in photoprotection to minimise photodamage, or allow for photodamage to occur and invest in photorepair; however, the relative contribution of photoprotection and photorepair remains uncharacterised. Here we determined the light dependence of Photosystem II (PSII) photoinhibition and photorepair in 2 phylotypes of *Symbiodinium* displaying different susceptibilities to thermal stress. Upon exposure to photon flux densities (PFDs) >500 µmol photons m^{-2} s^{-1} the thermally 'sensitive' Strain A1.1 displayed higher net photoinhibition, measured as a decrease in maximum PSII efficiency (F_v/F_m), than the thermally 'tolerant' Strain A1. In contrast, gross photoinhibition, assessed as the decline of F_v/F_m in the presence of an inhibitor of D1 protein synthesis, was similar in the 2 strains. Therefore, photorepair was considered to be the key mechanism minimising net photoinhibition in Strain A1. Consistent with this conclusion, the 2 strains displayed similar capacities for other mechanisms of avoiding photodamage, specifically, photochemical (q_P) and non-photochemical (NPQ) excitation energy quenching. Measurements on Strain A1 grown under 2 PFDs (100 and 650 µmol photons m^{-2} s^{-1}) revealed that photoacclimation to HL involved the upregulation of q_P, which minimised gross photoinhibition by maintaining PSII in a more oxidised state. We conclude that both interspecific (e.g. phylotype diversity) and intraspecific (e.g. photoacclimation state) factors affect the susceptibility of *Symbiodinium* to light stress.

KEY WORDS: *Symbiodinium* · Photoinhibition · Photorepair · PSII antenna · Variable fluorescence · Xanthophyll cycle

INTRODUCTION

Reef-building corals and many other cnidarians rely on symbiotic microalgae to provide much of their nutrition in low nutrient waters. Consequently, growth, distribution and ultimately the success of corals are strongly dependent on light availability (Falkowski & Dubinsky 1981, Gorbunov et al. 2001, Hennige et al. 2009). For example, the ability of the algal symbionts to photoacclimatise to low photon flux densities (PFDs) constrains the lower depth distribution of corals (Gorbunov et al. 2001).

Recent attention has turned to how corals survive high light (HL) exposure (Salih et al. 2000, Iglesias-Prieto et al. 2004, Warner & Berry-Lowe 2006, McCabe Reynolds et al. 2008), since photoinhibition of photosynthetic electron transport induces photodamage to Photosystem II (PSII) and consequent production of damaging reactive oxygen species (ROS) in *Symbiodinium* spp. (Smith et al. 2005). This process is also observed when *Symbiodinium* is heat-stressed (e.g. Lesser & Farrell 2004, Tchernov et al. 2004, Robison & Warner 2006, Suggett et al. 2008). Several studies have demonstrated temperature-dependent loss of PSII ac-

*Email: mragni@essex.ac.uk

tivity (and a concomitant decrease in the D1 protein), both when *Symbiodinium* occurs *in hospite* of the coral and when *Symbiodinium* is cultured *in vivo* (Warner et al. 1999, Takahashi et al. 2004, 2008). Further work has demonstrated that the rate of the thermally dependent loss of PSII and of PSII activity is determined by light intensity. Higher PFDs exacerbate the effect of thermal stress (Lesser & Farrell 2004, Robison & Warner 2006), presumably because both factors act cumulatively to damage PSII (Smith et al. 2005). Consequently, examining the response of *Symbiodinium* strains to HL intensities may provide insight into mechanisms underlying the coral bleaching phenomenon.

At any one time, PSII activity is a function of the net rates of photoprotection, photodamage and photorepair. Investing in photoprotection over photorepair likely has very different implications for minimising long-term damage from HL. As yet the relative 'investment' by *Symbiodinium* in one mechanism over the other is unknown. Nonetheless, we can speculate that the ability of zooxanthellae to withstand exposure to HL may constrain the growth of corals within shallow water and HL growth environments, which also experience high daily fluctuations in temperature.

The zooxanthellae endosymbionts of corals have developed several mechanisms to cope with high and variable light intensities through a suite of photoprotection mechanisms, including pigment and enzyme activity regulation (Levy et al. 2006). Consequently, these zooxanthellae may be able to continuously 'tune' their photophysiology in relation to the daily course of light and UV radiation. In zooxanthellae *in hospite*, as much as 80% of absorbed excitation energy can be dissipated by non-photochemical quenching (NPQ), i.e. the dissipation of energy as heat, rather than being passed onto the PSII reaction centres (RCIIs) for photochemistry (Gorbunov et al. 2001). NPQ via xanthophyll cycling (XC) is amongst the most efficient photoprotective mechanisms in marine microalgae and consists of the light-promoted conversion of pigment diadinoxanthin (ddx) into diatoxanthin (dtx), which allows absorbed light energy (excitation energy) to be dissipated within the light-harvesting antenna (Arsalane et al. 1994, Olaizola et al. 1994). Indeed, significant shifts in dtx:ddx ratios have been observed for *Symbiodinium* spp. in response to the daily increase of light and reduction in the effective quantum efficiency of PSII (Brown et al. 1999, Warner & Berry-Lowe 2006). Despite these observations, Venn et al. (2006) questioned the importance of XC as a protective mechanism in coral bleaching, and noted no correlation between susceptibility to temperature/irradiance stress and pigment composition.

In spite of the substantial investment in photoprotection, the RCII protein D1 remains one of the main targets of PSII photodamage (Adir et al. 2003), and the rate of D1 damage increases with exposure to HL. Although photodamage can occur under any light intensity, photoinhibition is observed only when the rate of damage exceeds the rate of repair (Adir et al. 2003). HL alone has been reported to photoinhibit up to 30 to 40% of the PSII activity in shallow water corals even at moderate temperatures (24 to 29°C) (Gorbunov et al. 2001). Most of the inactive RCII are generally repaired within hours following transfer back to low light (LL) intensities. However, a proportion (10 to 20%) of the RCIIs appears to be chronically photoinhibited (Gorbunov et al. 2001, Warner et al. 2002). This proportion may vary throughout the year, with evidence for seasonality in photoinactivation and photoacclimation (Gorbunov et al. 2001, Warner et al. 2002), and may vary as well between symbionts of shallow water corals and those living at depth, with important implications on the effects on photosynthesis. Specifically, the effect of photoinhibition on the photosynthetic rate is likely to be more severe in light-limited than in light-saturated populations (Behrenfeld et al. 1998). Therefore, photorepair plays a critical role in mitigating the overall net photoinhibition rate and potentially in contributing to the long-term stability of coral-algal symbioses.

Heat stress experiments on *Symbiodinium* both *in hospite* and *in vivo* have also demonstrated the mediating role of photorepair. Warner et al. (1999) hypothesised that variation in PSII repair accounted for variability in bleaching susceptibility. Further work corroborated this notion by demonstrating that decreased rates of repair of photodamaged PSII accelerated photoinhibition by heat stress and thus partly determined the sensitivity of corals to thermal bleaching (Yakovleva & Hidaka 2004, Takahashi et al. 2004, 2009, Takahashi & Murata 2008). However, these previous studies have not provided direct information on the light-dependence of damage and repair rates of RCIIs, which both determine *Symbiodinium* susceptibility to further stress (e.g. heat stress). Importantly, researchers examining bleaching now recognise that the *Symbiodinium* genus is comprised of numerous genetically distinct 'types' that exhibit differential tolerance to thermal stress and RCII loss (e.g. Tchernov et al. 2004, Robison & Warner 2006, Suggett et al. 2008, Takahashi & Murata 2008), although it is not yet known whether these differences in stress tolerance can be accounted for by differences in rates of RCII damage and repair.

The first objective of the present study was to provide for the first time quantitative rates of photoinhibition and photorepair for a thermally 'tolerant' and a 'sensitive' strain of *Symbiodinium* to acute exposure to a wide range of light intensities. We used fluorescence-

based methods to determine the rates of PSII photoinhibition and photorepair, and changes in the PSII antenna size (σ_{PSII}), electron transport rates (ETR^{RCII}), and photochemical quenching (q_P) and NPQ. Rates of damage and repair were discriminated by incubating samples in the presence and absence of a chloroplast protein synthesis inhibitor, lincomycin (Lesser et al. 1994, Warner et al. 1999, Bouchard et al. 2005, Ragni et al. 2008), since it blocks *de novo* synthesis of the D1 protein and thus prevents the replacement of the damaged protein during the PSII repair cycle.

The second objective was to assess the relative role of photoprotection and photorepair in counteracting photodamage as a function of the photoacclimation state of *Symbiodinium*. For this purpose, the response of the 'tolerant' strain was also examined in relation to the growth irradiance of the culture. Concurrent changes in the pigment composition, including XC pigments, were analysed so as to provide additional insights into the mechanism(s) of photoprotection.

MATERIALS AND METHODS

Culture. Semi-continuous cultures of *Symbiodinium* A1 and A1.1 (designated by ITS2 nomenclature, LaJeunesse 2001), thermally tolerant and sensitive strains, respectively (Robison & Warner 2006), were grown at 26°C in 0.2 µm filtered artificial seawater medium ASP-8A (Provasoli et al. 1957) as described in Hennige et al. (2009). Cell concentrations were monitored daily using improved Neubauer haemocytometers (Marienfeld) and diluted to maintain cells in exponential growth phase at a target density of ~50 000 cells ml^{-1}. Light was provided in 14 h light:10 h dark cycles by cool white fluorescent tubes at 100 µmol photons m^{-2} s^{-1} (LL). Strain A1 was also grown at 650 µmol photons m^{-2} s^{-1} (HL), using an additional cool white fluorescent lamp.

Light-response experiments. Light-response experiments were used to determine the biophysical characteristics of PSII, in order to define the light dependence of PSII photoinhibition, photorepair and photoprotective processes. Aliquots of 300 ml were harvested from the growth chamber in the middle of the light period and distributed into 30 glass tubes (10 ml). The tubes were distributed along a light gradient in 3 parallel rows in an incubator cooled with a thermostatic bath set to the growth temperature and illuminated by a block of blue light-emitting diodes (LEDs; 465 nm peak height; see Fig. 1 in Ragni et al. 2008). We accounted for the differences in photosynthetically utilisable radiation (PUR) between the white fluorescent lamps used for growth and the blue LED by using a conversion factor calculated as described in Ragni et al. (2008). The PUR of the fluorescent light source was ca. 40% of that of the blue LED source. Hereafter we report PFD as white light-equivalent PFDs.

Each of the 10 tubes per row was simultaneously exposed for 2 h to 1 of 10 PFDs. Light exposure decreased exponentially from ca. 1600 to 5 µmol photons m^{-2} s^{-1} with increasing distance of the tubes from the LEDs. Scalar PFD was measured inside each tube using a spherical photosynthetically active radiation (PAR) sensor (Li-Cor, model Ll-250A). Aliquots of 3 ml were removed from 1 row of tubes for analysis of variable fluorescence at the start (t_0) and end (t_{0+2h}) of the experiment. Aliquots of 10 ml from a second row of tubes were also taken for pigment analysis but only for Strain A1 (HL and LL cultures). Experiments were repeated 3 times, on different sampling days on cultures of A1.1-LL, A1-LL and A1-HL.

Inhibitor treatment. Samples in the third row of tubes were incubated with lincomycin (Sigma Aldrich) in order to block D1 repair and evaluate gross photoinhibition, as explained below ('Dark-acclimated variable fluorescence'). The inhibitor of the D1 protein synthesis was added in the dark 20 min before the experiment to a final concentration of 0.9 mM (Bouchard et al. 2005, Ragni et al. 2008) and the cultures were then incubated along one of the rows of the incubator under the same light regimes as the non-treated samples. Aliquots of 3 ml were taken for variable fluorescence measurements after the 2 h incubation period.

Dark-acclimated variable fluorescence. Measurements were carried out at t_0 and t_{0+2h} (light-response experiments) after 35 to 45 min incubation in complete darkness, in order to allow the full reversal of NPQ (e.g. Suggett et al. 2003). Measurements were performed using a fluorescence induction and relaxation (FIRe) fluorometer (Satlantic). Excitation was provided by a high-luminosity blue and green LED array (450 and 500 nm peak heights, respectively). The measurement protocol was the same as described previously (Ragni et al. 2008, Suggett et al. 2008, Hennige et al. 2009). All measurements were made at instrument gains of 400 to 800 and modified so as to ensure the signal was between 50 to 70% of the upper detection limits; 16 iterations were performed per sample to further increase the signal:noise ratio.

The FIRe data processing was performed using the software FirePro (v. 1.20, Satlantic) provided with the instrument. The parameters retrieved from measurements performed in darkness were the minimum (F_0) and maximum (F_m) fluorescence yields, and the effective cross-section of PSII (σ_{PSII}). The maximum PSII efficiency was expressed as $F_v/F_m = (F_m - F_0)/F_m$.

Dark-acclimated measurements were carried out on all lincomycin-treated and untreated samples from each light level in order to characterise the effect of the

light treatment on the physiological potential for processing light. Comparative measures of F_v/F_m between lincomycin-treated and untreated samples after exposure to a range of PFDs were used to calculate the net and the gross photoinhibition rates (termed NPiR and GPiR, respectively) for each PFD using the following equations (Ragni et al. 2008):

$$\mathrm{NPiR}(E) = -\frac{\ln \frac{F_v/F_m(E)}{F_v/F_m(E_0)}}{\Delta T} \quad (1)$$

$$\mathrm{GPiR}(E) = -\frac{\ln \frac{F_v/F_{mLIN}(E)}{F_v/F_m(E_0)}}{\Delta T} \quad (2)$$

where E is the PFD applied; $F_v/F_m(E_0)$ is the F_v/F_m measured on the sample exposed to the lowest PFD; $F_v/F_m(E)$ are the values of F_v/F_m measured at the end of light exposure at different PFD levels E, on dark-acclimated samples; $F_v/F_{mLIN}(E)$ is the same parameter, measured on lincomycin-treated samples; ΔT is the duration in minutes of the light incubation period. All the rates are expressed in min^{-1}. These equations assume that the change in F_v/F_m occurs at a constant specific rate (e.g. $d(F_v/F_m)/dt = kF_v/F_m$) (Six et al. 2009). From the difference between these photoinhibition rates we calculated the repair rate (RR) as follows:

$$\mathrm{RR}(E) = \mathrm{GPiR}(E) - \mathrm{NPiR}(E) \quad (3)$$

Terms and definitions are summarised in Table 1.

Variable fluorescence measurements under actinic light. Variable fluorescence was also measured under actinic light, on separate samples, to determine the partitioning of light energy between photochemistry and thermal dissipation. For this purpose light-response curves were carried out in triplicate for each culture. Aliquots of 3 ml were taken directly from the growth vessel, dark-acclimated for 40 min and then placed in the cuvette holder of the FIRe, which was illuminated by a blue actinic light source module (ALS, Satlantic). Samples were progressively exposed to 10 increasing PFDs between 0 and 1000 µmol photons m^{-2} s^{-1}. Each PFD was delivered for 4 min and variable fluorescence was measured during the final minute of illumination at each of these PFDs.

The parameters retrieved from this set of measurements were F', F_m' and σ'_{PSII} (see Table 1). The PSII operating efficiency was expressed as: $F_q'/F_m' = (F_m' - F')/F_m'$. q_P was calculated as $(F_m' - F')/(F_m' - F_0')$, where F_0' was derived from measurements of F_0, F_m and F_m' (Baker & Oxborough 2004, our Table 1). NPQ was quantified as $(F_m - F_m')/F_m'$, according to the Stern-Volmer equation (Bilger & Björkman 1990). ETR^{RCII} (mol e^- mol $RCII^{-1}$ h^{-1}) was determined as:

$$\mathrm{ETR}^{\mathrm{RCII}} = \mathrm{PFD} \cdot \sigma_{PSII} \cdot F_q'/F_m' \cdot 21.683 \quad (4)$$

where σ_{PSII} is the value of the effective cross-section measured on the dark-acclimated sample, and the factor 21.683 converts seconds to hours, µmol e^- to mol e^- and $Å^2 \cdot \mathrm{quantum}^{-1}$ to $m^2 \cdot \mathrm{mol\ RCII}^{-1}$ (Suggett et al. 2003, 2006).

Pigment determinations. Pigment samples were collected on HL and LL cultures of Strain A1 prior to light-response experiments and immediately after incubation for 2 h at a range of PFDs. Samples (10 ml) were filtered immediately on 25 mm GF/F filters (Whatman), in order to prevent the reversal of the XC; filters were flash-frozen in liquid N_2, and stored at −80°C until analysis. Pigments were extracted from GF/F filters in 100% acetone and analysed by HPLC using a reversed-phase C8 column and gradient elution (Barlow et al. 1997) on an Agilent 1100 Series HPLC system (more details in Ragni et al. 2008).

We classified the detected pigments as photosynthetic (PSP) or non-photosynthetic pigments (Table 1). PSP include chlorophylls (chl *a*, chl c_2) and the photosynthetic carotenoid peridinin (per). Non-photosynthetic pigments, hereinafter referred to as photoprotective carotenoids (PPC), include β,β-carotene (βcar), ddx, dtx and dinoxanthin (dnx). Amongst the PPCs, ddx and dtx are classified as XC pigments and the ratio dtx/(ddx + dtx) as de-epoxidation state index (DPS), which is an indicator of the extent of XC.

Statistical analysis. The statistical analysis was performed using GraphPad InStat v. 3.10 for Windows. The significance of the results was assessed by 1-way ANOVA when the ANOVA conditions were satisfied, i.e. when the data sets to compare were 3 in number. The variables tested were: F_v/F_m, σ_{PSII}, GPiR, NPiR, RR, NPQ and q_P, collected in triplicates on 3 culture sets. The factor tested was the difference between cultures (i.e. 2 genetically different cultures plus the HL-grown culture). When p from ANOVA was <0.05, the post hoc Tukey's multiple comparison test was applied in order to determine which of the means were different from the others.

When the data sets to compare were only 2 in number, an unpaired *t*-test was used. The variables tested were pigment ratios (measured on 2 sets of cultures, in triplicates) and the above-mentioned fluorescence parameters, when compared within the same culture. In the former case the factor tested was the growth irradiance (i.e. HL- vs. LL-grown culture), while in the latter case the tested factor was the actinic PFD exposure. Curve-fitting and linear least-squares regression analysis were performed using the software Grapher v. 4.0 (Golden Software) in order to characterise the pigments versus PFD dependencies and the relationship between σ_{PSII} and F_v/F_m.

Table 1. Terms, definitions and units of measurements used in the present study

Term	Definition	Derivation	Units
βcar	β,β-carotene	–	ng l^{-1}
chl *a*	Chlorophyll *a*	–	ng l^{-1}
chl c_2	Chlorophyll c_2	–	ng l^{-1}
ddx	Diadinoxanthin	–	ng l^{-1}
dnx	Dinoxanthin	–	ng l^{-1}
dtx	Diatoxanthin	–	ng l^{-1}
DPS	De-epoxidation state	dtx/(ddx + dtx)	Dimensionless
E	The PFD applied	–	µmol photons m^{-2} s^{-1}
ETR^{RCII}	Electron transport rate	Eq. (4)	mol e^- mol $RCII^{-1}$ h^{-1}
F_0, F_m	Minimum and maximum fluorescence measured in darkness	–	Instrument units
F_0'	Minimum fluorescence under actinic light	$\frac{F_0}{F_v/F_m + F_0/F_m'}$	Instrument units
F'	Steady-state fluorescence measured at any point, under actinic light	–	Instrument units
F_m'	Maximum fluorescence under actinic light	–	Instrument units
F_q'	Difference between F_m' and F'	$F_m' - F'$	Instrument units
F_v, F_v'	Variable fluorescence in darkness, and under actinic light	$F_m - F_0$, $F_m' - F_0'$	Instrument units
F_v/F_m, F_v'/F_m'	PSII maximum photochemical efficiency in a dark-acclimated state, and under actinic light	$(F_m - F_0)/F_m$, $(F_m' - F_0')/F_m'$	Dimensionless
F_q'/F_m'	PSII operating efficiency under actinic light	$(F_m' - F')/F_m' = F_v'/F_m'$, F_q'/F_v'	Dimensionless
NPiR, GPiR	Net and gross photoinhibition rate	Eqs. (1) & (2)	min^{-1}
NPQ	Non-photochemical quenching coefficient	$(F_m/F_m') - 1$	Dimensionless
per	Peridinin	–	ng l^{-1}
PFD	Photon flux density	–	µmol photons m^{-2} s^{-1}
q_P	Photochemical quenching, or PSII efficiency factor under actinic light	$F_q'/F_v' = (F_m' - F')/(F_m' - F_0')$	Dimensionless
RR	Repair rate	Eq. (3)	min^{-1}
σ_{PSII}, σ'_{PSII}	Effective absorption cross section of PSII in darkness, and under actinic light	–	$Å^2$ q^{-1}
ΣXC	Total xanthophyll cycle pigments pool	ddx + dtx	ng l^{-1}
ΣPPC	Total photoprotective carotenoids pool	chl *a* + chl c_2 + per	ng l^{-1}
ΣPSP	Total photosynthetic pigments pool	βcar + ddx + dtx + dnx	ng l^{-1}

RESULTS

Photoinhibition and photorepair

Values of F_v/F_m measured at the beginning of the light-response experiment (t_0) were similar for all the cultures (Fig. 1a–c, Table 2). After 2 h of exposure to different PFDs, F_v/F_m decreased with increasing light in LL cultures; this decrease was greater for A1.1 than for A1 culture (41% vs. 25% at ~1600 µmol photons m^{-2} s^{-1}; Fig. 1a,b, Table 2). Furthermore, the light-induced decrease in F_v/F_m was observed at lower PFDs for A1.1 than for A1. In contrast, A1-HL acclimated cells did not exhibit any significant light induced change in F_v/F_m (Fig. 1c).

As expected, lincomycin-treated samples displayed a more pronounced light-dependent reduction in F_v/F_m in all the cultures as a result of the inhibition of D1 repair. However, the differences between F_v/F_m measured on treated and non-treated samples were greater for Strain A1 than for A1.1 (Fig. 1a–c), indicating that more repair had occurred in the thermally tolerant strain (see RR in Table 2). Rates of photoinhibition and repair were quantified by applying Eqs. (1) to (3) for each exposure PFD.

LL-acclimated cultures of both Strains A.1 and A.1.1 displayed similar light dependence of GPiR, indicating similar susceptibilities to light-induced damage (Fig. 2a, Table 2). In contrast, NPiR was about 2-fold higher for A1 than A1.1 (Fig. 2b, Table 2). Whereas GPiR increased as the square root of PFD (Fig. 2a), NPiR increased linearly with PFD (Fig. 2b).

The light dependence of both GPiR and NPiR was significantly affected by growth under HL in Strain A1, the only strain for which we have data at HL. Specifically, GPiR was up to 4-fold lower for the HL- than LL-grown A1 culture (Fig. 2a, Table 2), and NPiR was close to zero (i.e. no net photoinhibition) for the A1-HL culture over the whole light range applied.

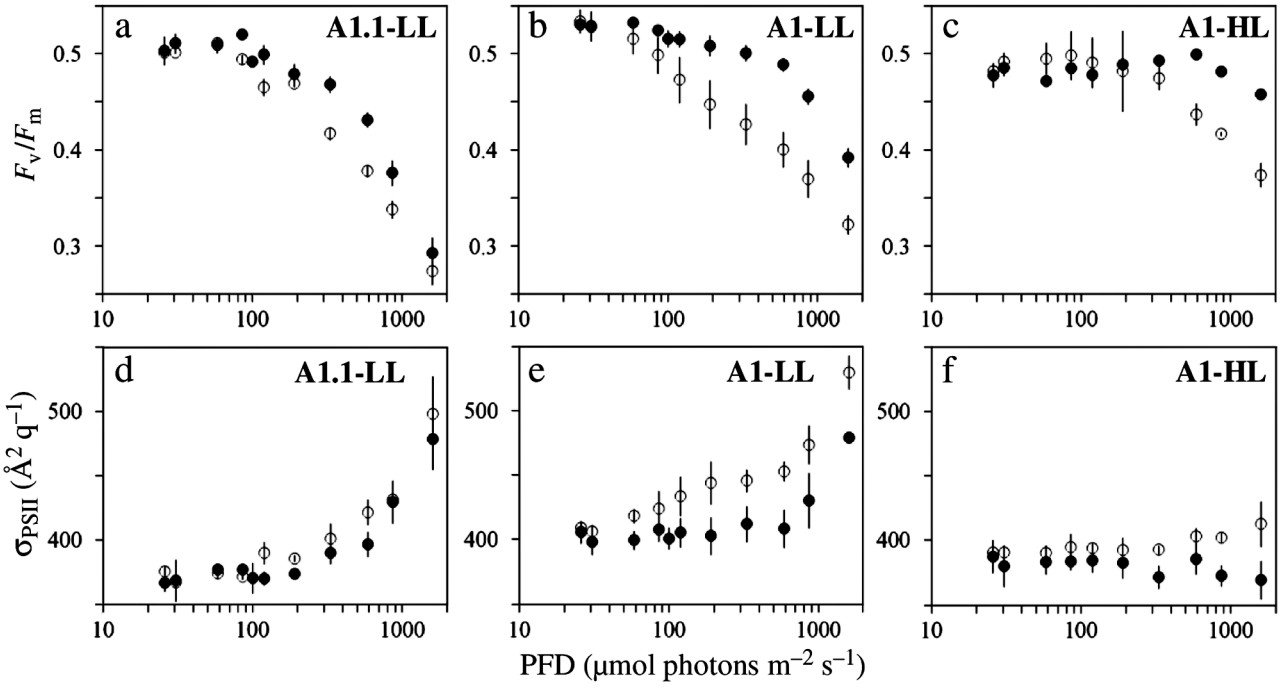

Fig. 1. *Symbiodinium*. (a–c) Light dependence of PSII maximum photochemical efficiency (F_v/F_m) and (d–f) PSII effective cross-section (σ_{PSII}) measured with a FIRe fluorometer after 2 h exposure to different PFD (light-response experiments) on dark-acclimated samples. ○: lincomycin-treated samples, ●: untreated samples. Data are mean ±SE (n = 3)

Table 2. *Symbiodinium*. Variable fluorescence-derived parameters (mean ± SE) measured on the 3 cultures at their growth PFD (100 µmol photons m^{-2} s^{-1} for LL-acclimated cultures and 650 µmol photons m^{-2} s^{-1} for HL-acclimated cultures) and at the maximum actinic PFD applied during light-response experiments (ca. 1600 µmol photons m^{-2} s^{-1}) (units for each variable are dimensionless unless indicated otherwise), and results from 1-way ANOVA performed across the 3 cultures. Superscript letters indicate groupings as determined from the ANOVA post hoc Tukey's test (when $p < 0.05$). Different letters indicate significant difference, while the same letter indicates no difference

	PFD	Culture			1-way ANOVA	
		A1.1 LL	A1 LL	A1 HL	$F_{2,6}$	p
F_v/F_m	Growth	0.499 ± 0.006	0.516 ± 0.008	0.499 ± 0.002	1.87	0.237
	Max.	0.353 ± 0.03 ^{A}	0.392 ± 0.009 ^{A,B}	0.458 ± 0.005 ^{B}	6.23	0.034
σ_{PSII} (Å^2 q^{-1})	Growth	370 ± 14.2	400 ± 7.99	384 ± 9.02	3.62	0.093
	Max.	478 ± 23.4 ^{A}	479 ± 3.53 ^{A}	369 ± 14.5 ^{B}	6.27	0.034
GPiR (min^{-1})	Growth	$6.55 \times 10^{-4} \pm 7.59 \times 10^{-5}$	$9.54 \times 10^{-4} \pm 4.57 \times 10^{-4}$	$1.91 \times 10^{-4} \pm 4.32 \times 10^{-4}$	2.98	0.126
	Max.	$5.06 \times 10^{-3} \pm 7.59 \times 10^{-4}$ ^{A}	$4.14 \times 10^{-3} \pm 2.52 \times 10^{-4}$ ^{A}	$1.27 \times 10^{-3} \pm 4.99 \times 10^{-4}$ ^{B}	13.2	0.006
NPiR (min^{-1})	Growth	$3.33 \times 10^{-5} \pm 2.54 \times 10^{-4}$	$2.39 \times 10^{-4} \pm 1.63 \times 10^{-4}$	$-1.25 \times 10^{-4} \pm 2.51 \times 10^{-4}$	0.270	0.77
	Max.	$4.47 \times 10^{-3} \pm 4.10 \times 10^{-4}$ ^{A}	$2.51 \times 10^{-3} \pm 2.14 \times 10^{-4}$ ^{B}	$6.90 \times 10^{-5} \pm 3.52 \times 10^{-4}$ ^{C}	43.2	0.0003
RR (min^{-1})	Growth	$6.21 \times 10^{-4} \pm 1.78 \times 10^{-4}$ ^{A,B}	$7.15 \times 10^{-4} \pm 3.00 \times 10^{-4}$ ^{A}	$3.16 \times 10^{-4} \pm 2.52 \times 10^{-4}$ ^{B}	5.74	0.041
	Max.	$5.92 \times 10^{-4} \pm 3.49 \times 10^{-4}$ ^{A}	$1.63 \times 10^{-3} \pm 9.59 \times 10^{-5}$ ^{B}	$1.20 \times 10^{-3} \pm 1.68 \times 10^{-4}$ ^{A,B}	5.54	0.043
NPQ	Growth	0.362 ± 0.042 ^{A}	0.257 ± 0.024 ^{A}	1.467 ± 0.042 ^{B}	24.1	0.001
	Max.	1.97 ± 0.045 ^{A}	2.51 ± 0.157 ^{B}	2.51 ± 0.059 ^{B}	15.6	0.004
q_P	Growth	0.884 ± 0.034	0.808 ± 0.014	0.909 ± 0.026	33.8	0.001
	Max.	0.459 ± 0.037 ^{A}	0.360 ± 0.015 ^{A}	0.891 ± 0.016 ^{B}	264	0.0001

RR increased linearly with PFD up to ca. 200 µmol photons m^{-2} s^{-1} ($r^2 > 0.96$, n = 18, curve fit not shown) in all the examined cultures (Fig. 2c). RR plateaued at ca. 800 µmol photons m^{-2} s^{-1} for Strain A1 (both HL and LL cells) and peaked at ca. 600 µmol photons m^{-2} s^{-1} for the thermally sensitive Strain A1.1. RR was more than 2-fold higher for Strain A1 than for A1.1 under the highest PFD (Table 2). Overall, the HL-grown Strain A1 culture displayed lower RRs for PFDs <800 µmol photons m^{-2} s^{-1}; however, these rates generally balanced the GPiR to result in zero net photoinhibition.

PSII antenna size

The σ_{PSII} cross-sections were the same for all strains prior to the experiments, ranging between 370 ± 14.2 and 400 ± 7.99 Å^2 q^{-1} (Fig. 1d–f, Table 2). Upon exposure to HL, σ_{PSII} increased by up to 20% for LL-grown Strain A1 cells and 30% for Strain A1.1 (Table 2), but did not significantly change for HL-grown A1 cells. Treatment with lincomycin induced a 10% increase in σ_{PSII} for LL-grown Strain A1 cells compared to untreated cells (t = 3.87, df = 4, $p < 0.05$), but not for Strain A1.1. A scatter plot of σ_{PSII} versus F_v/F_m (Fig. 3) from all samples and all conditions used in the present study yielded an inverse correlation for cultures grown under LL conditions (Fig. 3a,b, Table 3). This suggests a correlation between the extent of photoinhibition (decrease in F_v/F_m) and the increase in the PSII antenna size, as expected for a cumulative loss of RCIIs (see Suggett et al. 2009). In contrast, in the experiments employing cells grown under HL, the 2 parameters were not correlated (Fig. 3c, Table 3).

NPQ, q_P and ETR

The light-dependence of the NPQ coefficient, calculated from untreated samples, was similar for both Strains A1 and A1.1 (Fig. 4a). NPQ increased rapidly with increasing PFD, in particular between 0 and 400 µmol photons m^{-2} s^{-1}. However, the values of NPQ achieved at elevated PFDs were ca. 20% lower for the sensitive (A1.1) than for the tolerant (A1) strain (Table 2). Compared to the LL-grown cultures, the HL-grown A1 culture exhibited a different light-dependency of NPQ, generally increasing linearly with PFD and exhibiting lower values of NPQ for PFDs > 150 µmol photons m^{-2} s^{-1} ($t(4) = 3.94$, $p < 0.05$). Interestingly, the values of NPQ for this HL-grown culture converged with values of NPQ for the LL-grown culture at the highest-exposure PFD (Fig. 4a, Table 2), suggesting differential operation of the photoprotective mechanisms to light exposure.

The light-dependence of q_P was comparable for the 2 strains grown under LL (Fig. 4b, Table 2): q_P declined by only ca. 20% at PFDs < 200 µmol photons m^{-2} s^{-1} ($t(4) = 3.60$, $p < 0.05$) but by as much as 60% at the highest-exposure PFDs ($t(4) = 12.83$, $p < 0.001$). In contrast, the HL-grown A1 culture exhibited no significant changes in q_P over the whole light regime applied (Fig. 4b, Table 2). Finally, values for ETR^{RCII} were similar in the 2 LL cultures (Fig. 4c), increasing linearly at PFDs < 200 µmol photons m^{-2} s^{-1} and saturating around 400 µmol photons m^{-2} s^{-1}. In contrast, the HL-grown culture exhibited up to 2-fold higher values of ETR^{RCII} compared to the LL-grown cultures and did not appear to saturate.

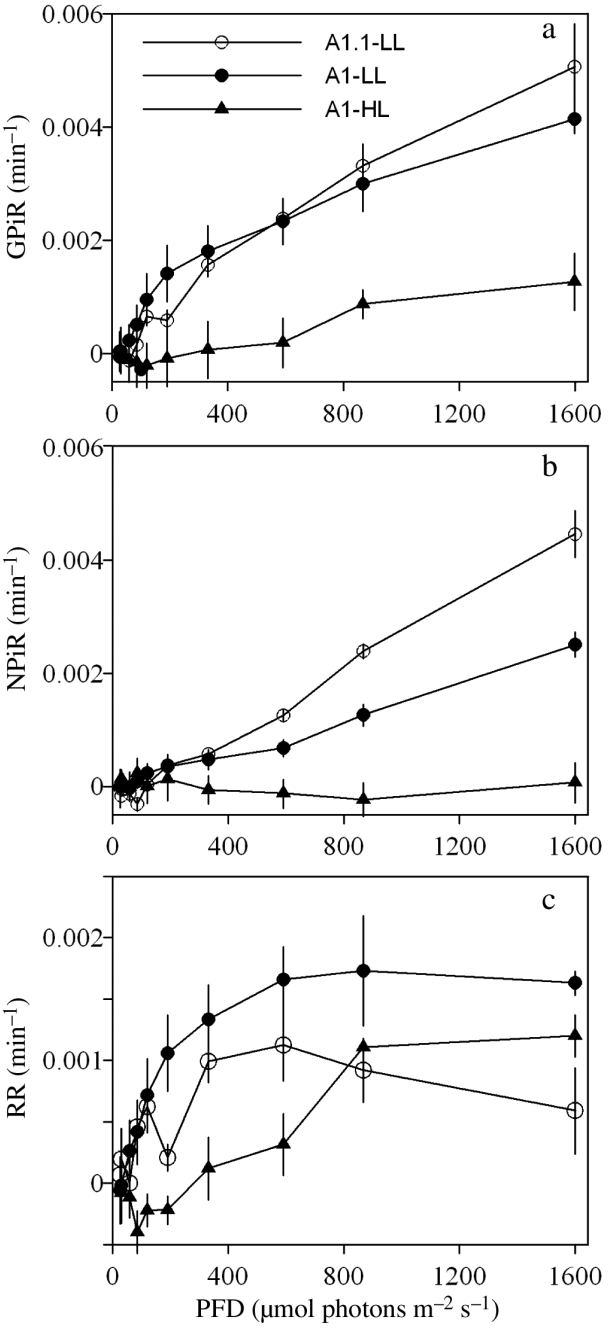

Fig. 2. *Symbiodinium*. Light dependence of (a) gross photoinhibition rate (GPiR), (b) net photoinhibition rate (NPiR) and (c) repair rate (RR) for Strains A1.1-LL (○), A1-LL (●) and A1-HL (▲). GPiR, NPiR and RR were calculated from data in Fig.1a–c, using Eqs. (1) to (3)

Pigment composition

The pigment profile of the HL and LL A1 cultures at t_0 (Fig. 5; t_0 values [□] plotted versus growth PFD) demonstrates the alternative photoacclimation states between LL and HL growth conditions. HL-grown cells

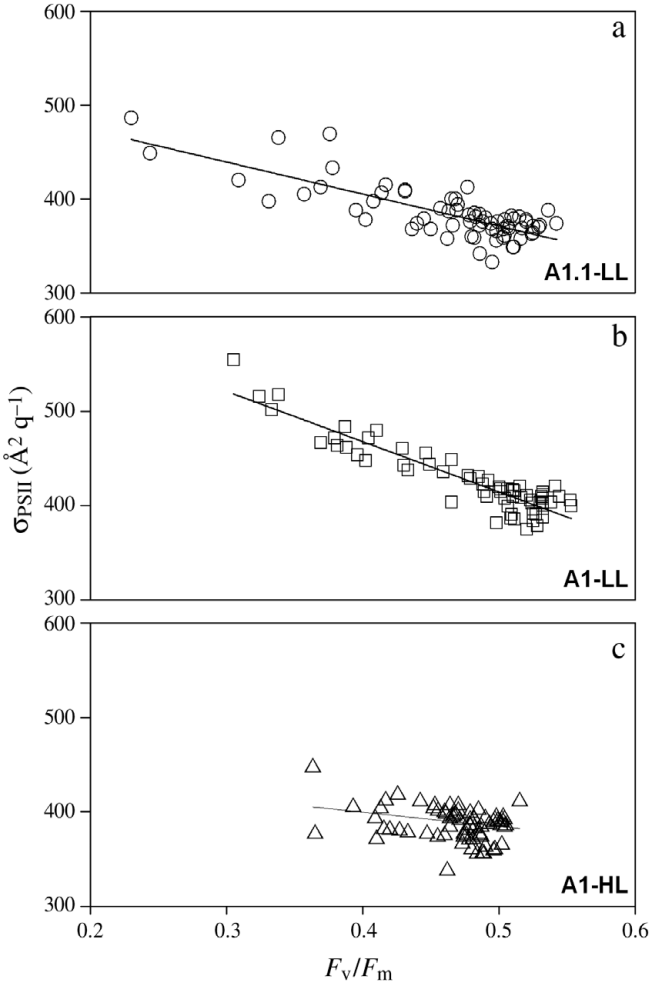

Fig. 3. *Symbiodinium*. Scatter plots of σ_{PSII} versus F_v/F_m measured on dark-acclimated samples for Strains (a) A1.1-LL (○), (b) A1-LL (□) and (c) A1-HL(△) with the FIRe fluorometer. Details on the fit are in Table 3

displayed a 2.5 times higher ratio of photoprotective to photosynthetic pigments (ΣPPC:ΣPSP, w:w) than LL-grown cells (Fig. 5a, Table 4). Cellular chl *a* concentration was about 2-fold higher in LL than HL cells (data not shown, but see Hennige et al. 2009). The chl *a*-normalised concentrations of light-harvesting pigments were higher for LL-grown cells, with per:chl *a* and chl c_2:chl *a* (w:w) being ca. 2- and 1.4-fold higher for LL than for HL cells, respectively (Fig. 5b,c, Table 4). In contrast, the ratios of PPCs to chl *a* were higher for HL than LL cells, in particular dnx:chl *a* and ΣXC:chl *a* (w:w) by about 2-fold and βcar:chl *a* by ca. 1.4 (Fig. 5d–f, Table 4).

The ratios of PSPs to chl *a* were unaffected by 2 h exposures over a gradient of PFDs from 10 to 1600 µmol photons m^{-2} s^{-1} in both the LL and HL cultures (Fig. 5b,c, Table 4). In contrast, the ratios of PPCs to chl *a* showed pronounced light dependence in both HL and LL cells (Fig. 5d–f, Table 4). Specifically, dnx:chl *a* increased with PFD according to a logarithmic function for HL-acclimated cultures (Table 3), achieving a 43% increase from the lowest to the highest PFD ($t(4) = 3.90$, $p < 0.05$), whereas it did not significantly change in LL cells. In contrast, βcar:chl *a* increased linearly with PFD (Table 3), by up to 30% in the LL culture ($t(4) = 4.26$, $p < 0.05$) and to 18% in the HL ($t(4) = 3.02$, $p < 0.05$).

XC pigments

The total xanthophyll-to-chl *a* ratio (ΣXC:chl *a*) was higher for HL- than for LL-grown cells (Fig. 5d) as a result of a higher concentration of ddx (Fig. 6a, Table 4). The light-response experiment revealed different patterns of interconversion of the XC pigments ddx and dtx for the 2 cultures (Fig. 6a,b). Specifically,

Table 3. Linear regression analysis results relative to the fit of pairs of parameters with the indicated function. Curve fits are shown in Fig. 3 (σ_{PSII} vs. F_m/F_v), Fig. 5 (ΣPPC:ΣPSP, dnx:chl *a*, βcar:chl a vs. PFD) and Fig. 6 (ΣXC, dtx:chl *a*, DPS vs. PFD)

Parameter	Culture	Fit equation	n	r^2	Residual mean square
σ_{PSII} vs. F_m/F_v	A1.1 LL	Linear $y = -340\ x + 541$	71	0.611	312
σ_{PSII} vs. F_m/F_v	A1 LL	Linear $y = -534\ x + 681$	67	0.840	213
σ_{PSII} vs. F_m/F_v	A1 HL	Linear $y = -151\ x + 460$	83	0.081	268
ΣPPC:ΣPSP vs. PFD	A1 HL	Linear $y = 5.02 \times 10^{-5}\ x + 0.317$	24	0.982	1.51×10^{-5}
	A1 LL	Log $y = 0.015 \ln(x) + 0.098$	24	0.936	2.36×10^{-5}
dnx:chl *a* vs. PFD	A1 HL	Log $y = 0.008 \ln(x) + 0.031$	24	0.966	3.92×10^{-6}
βcar:chl *a* vs. PFD	A1 HL	Linear $y = 3.84 \times 10^{-6}\ x + 0.034$	24	0.844	9.00×10^{-7}
	A1 LL	Linear $y = 5.10 \times 10^{-6}\ x + 0.027$	24	0.989	5.65×10^{-7}
ΣXC vs. PFD	A1 HL	Linear $y = 4.33 \times 10^{-5}\ x + 0.360$	24	0.944	3.62×10^{-5}
	A1 LL	Log $y = 0.025 \ln(x) + 0.105$	24	0.930	7.66×10^{-5}
dtx:chl *a* vs. PFD	A1 HL	Exponential $\ln(y) = 0.001\ x - 3.23$	24	0.988	0.005
	A1 LL	Log $y = 0.047 \ln(x) - 0.202$	24	0.963	1.34×10^{-4}
DPS vs. PFD	A1 HL	Exponential $\ln(y) = 0.001\ x - 2.21$	24	0.986	0.004
	A1 LL	Log $y = 0.166 \ln(x) - 0.707$	24	0.976	0.001

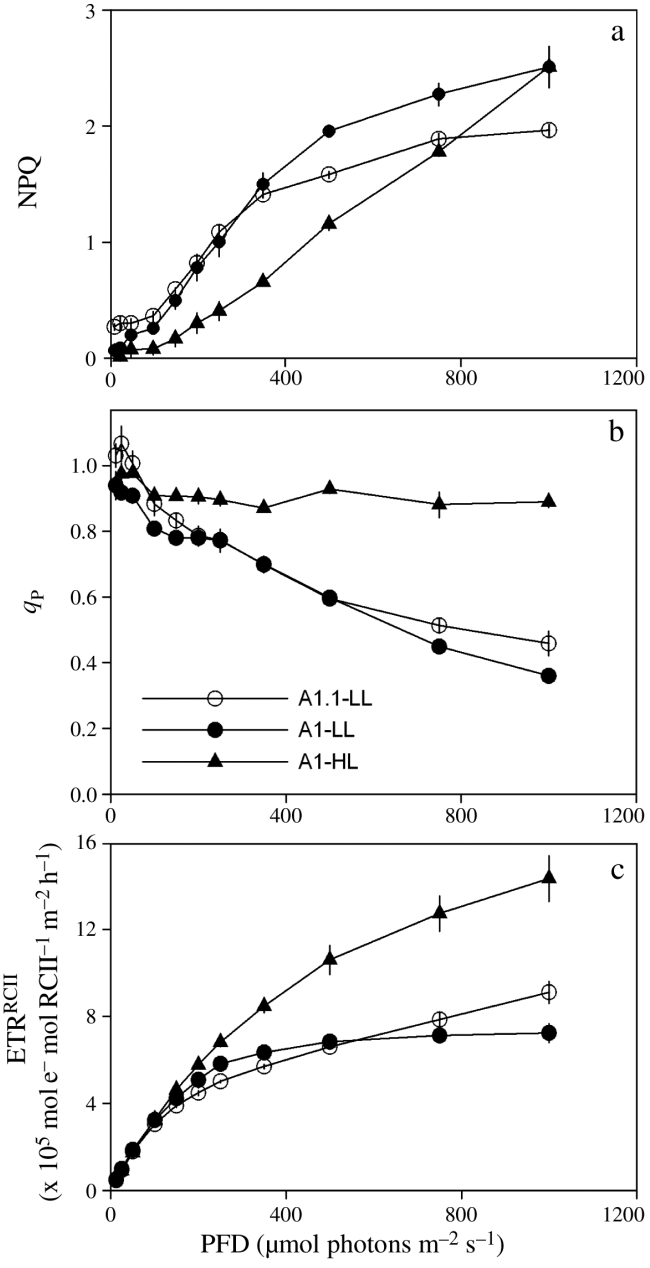

Fig. 4. *Symbiodinium*. Light dependence of fluorescence-derived parameters (a) photochemical quenching (q_P), (b) non-photochemical quenching (NPQ) and (c) RCII-specific electron transport rate (ETR^{RCII}), measured in the light (light-response curves) for Strains A1.1-LL (○), A1-LL (●) and A1-HL (▲). Data are mean ± SE (n = 3)

dtx:chl *a* increased with light according to a logarithmic function for LL-grown cells but followed an exponential function for HL-grown cells (Table 3). In contrast, ddx:chl *a* showed a similar pattern of decrease at high PFD in the 2 cultures. The PFD dependence of DPS (Fig. 6c, Table 3) closely resembled the pattern observed for dtx:chl *a*, indicating (1) an initial linear light-dependence of the conversion of ddx to dtx at low- to medium-exposure PFDs that plateaued at higher PFD for LL cultures, and (2) a higher efficiency in the conversion of ddx into dtx at high-exposure PFDs for HL-grown cells. After exposure to the lowest PFDs the DPS was 1 order of magnitude greater in HL cells than in LL cells, whereas after exposure to the highest PFD, the values of DPS in the 2 cultures converged to similar values (Fig. 6c, Table 4), and at intermediate values of PFD, LL cells displayed higher values of DPS.

DISCUSSION

Data presented here shed more light on the mechanisms employed by *Symbiodinium* to cope with supra-optimal (i.e. photoinhibiting) PFDs, and thus help us to understand how and to what extent these mechanisms vary between different phylotypes and/or between alternative photoacclimative states.

Strain-specific photodamage and photorepair

The finding that GPiR was similar for the 2 strains when grown under LL conditions indicates that they have similar susceptibilities to damage induced by acute HL exposure. However, the differences in the light dependence of NPiR indicates that these strains exhibit inherent differences in their ability to recover from the damage incurred. Although the actual PSII inactivation/damage experienced under HL was similar, the D1 repair cycle was faster (>2-fold) in the tolerant Strain A.1.1, which resulted in a lower NPiR. Our experiments thus demonstrate that the repair cycle is the key mechanism that minimises photoinhibition (and thus conveys 'tolerance') for Strain A1 compared to Strain A1.1.

Our data support the observations of Warner et al. (1999), who noted a greater PSII repair rate in another thermally tolerant strain of *Symbiodinium* (ITS type A3 originally from a giant clam) after acute heating, while they only partially confirm the observation of Takahashi & Murata (2008) that photorepair is suppressed under conditions which act to downregulate photosynthesis. Our observations imply that this is only the case for stress-sensitive phylotypes whose repair is inhibited under high irradiance. In fact, the tolerant strain achieved a 2-fold higher repair rate than the sensitive strain, showing the same extent of downregulation of photochemistry (i.e. decrease in q_P), the same biophysical characteristics (e.g. σ_{PSII}) and only a 20% higher extent of light dissipation through non-radiative pathways (NPQ). All the above indicates that both strains

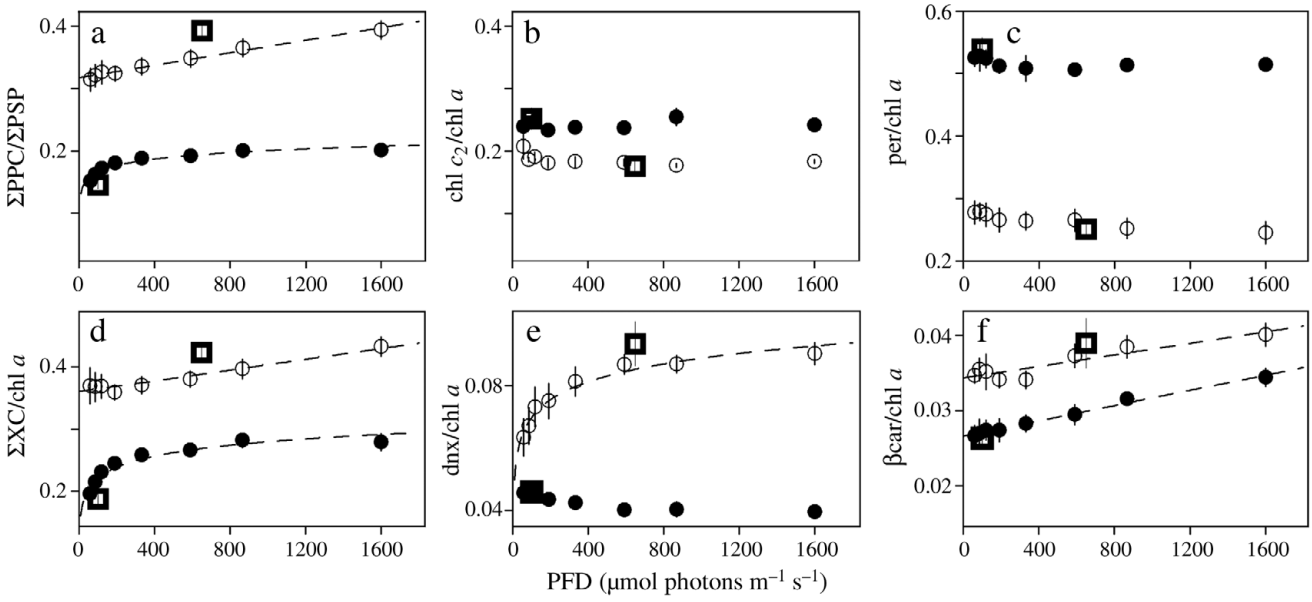

Fig. 5. *Symbiodinium*. Light dependence of photosynthetic and photoprotective pigment ratios (w:w) (a) ΣPPC:ΣPSP, (b) chl c_2: chl *a*, (c) per:chl *a*, (d) ΣXC:chl *a*, (e) dnx:chl *a* and (f) βcar:chl *a*, for Strains A1-HL (○) and A1-LL (●), measured after 2 h exposure to different PFDs (light-response experiments), and at t_0 (data plotted versus growth PFD, □). Data are mean ± SE (n = 3). Details on the fits are in Table 3

Table 4. *Symbiodinium*. Mean ± SE of pigment ratios measured on A1 cultures at their growth PFD (100 µmol photons m^{-2} s^{-1} for LL-acclimated cultures and 650 µmol photons m^{-2} s^{-1} for HL-acclimated cultures) and at the maximum actinic PFD applied during light-response experiments (ca. 1600 µmol photons m^{-2} s^{-1}), and results from the *t*-test

	PFD	Culture		Unpaired *t*-test	
		A1-HL	A1-LL	*t* (4)	p
chl c_2:chl *a*	Growth	0.182 ± 0.005	0.248 ± 0.002	11.50	0.0003
	Max.	0.184 ± 0.002	0.241 ± 0.006	9.40	0.0007
per:chl *a*	Growth	0.265 ± 0.018	0.524 ± 0.014	11.41	0.0003
	Max.	0.246 ± 0.017	0.515 ± 0.008	13.85	0.0002
dnx:chl *a*	Growth	0.087 ± 0.003	0.046 ± 0.001	12.22	0.0003
	Max.	0.090 ± 0.003	0.040 ± 0.001	13.87	0.0002
βcar:chl *a*	Growth	0.037 ± 0.002	0.027 ± 0.001	4.92	0.008
	Max.	0.040 ± 0.002	0.034 ± 0.001	2.95	0.0420
ddx:chl *a*	Growth	0.302 ± 0.008	0.217 ± 0.007	8.02	0.0013
	Max.	0.212 ± 0.010	0.128 ± 0.003	7.93	0.0014
dtx:chl *a*	Growth	0.078 ± 0.009	0.015 ± 0.002	6.60	0.0027
	Max.	0.221 ± 0.024	0.152 ± 0.012	2.56	0.0625
DPS	Growth	0.064 ± 0.007	0.204 ± 0.020	6.57	0.0028
	Max.	0.542 ± 0.019	0.507 ± 0.040	0.767	0.4860
ΣPPC:ΣPSP	Growth	0.392 ± 0.014	0.145 ± 0.003	13.95	0.0002
	Max.	0.394 ± 0.014	0.201 ± 0.005	13.15	0.0003

possess similar capacities for other mechanisms of avoiding photodamage, and thus further confirms the importance of the repair capability in shaping the ultimate response of *Symbiodinium* to light stress.

Our results may also have implications for understanding the thermal bleaching phenomenon, since cellular targets of heat and light stress (e.g. RCII and light-harvesting complexes) appear to be similar. HL exposure exacerbates the thermal stress response of *Symbiodinium* (Lesser & Farrell 2004, Robison & Warner 2006); therefore, the 2-fold difference in NPiR displayed by the 2 strains under HL stress is consistent with the classification of Strains A1 and A1.1 as tolerant and sensitive, respectively, based on thermal stress experiments (Robison & Warner 2006).

Phenotypic acclimation of photodamage and photorepair

The comparison between measurements on HL- and LL-grown A1 cultures demonstrated that light history, i.e. photoacclimation, can also play a major role in controlling the ability to prevent photoinhibition. The lower achieved RR displayed by culture A1-HL does not signify a lower repair capacity but rather a lower repair requirement. Specifically, the upregulation of the maximum rate of photochemistry observed in A1-HL adapted cultures primarily led to a decrease of the actual damage under HL stress (i.e. decrease in GPiR). From this we conclude that photoacclimation to HL helps to minimise PSII damage, minimising GPiR

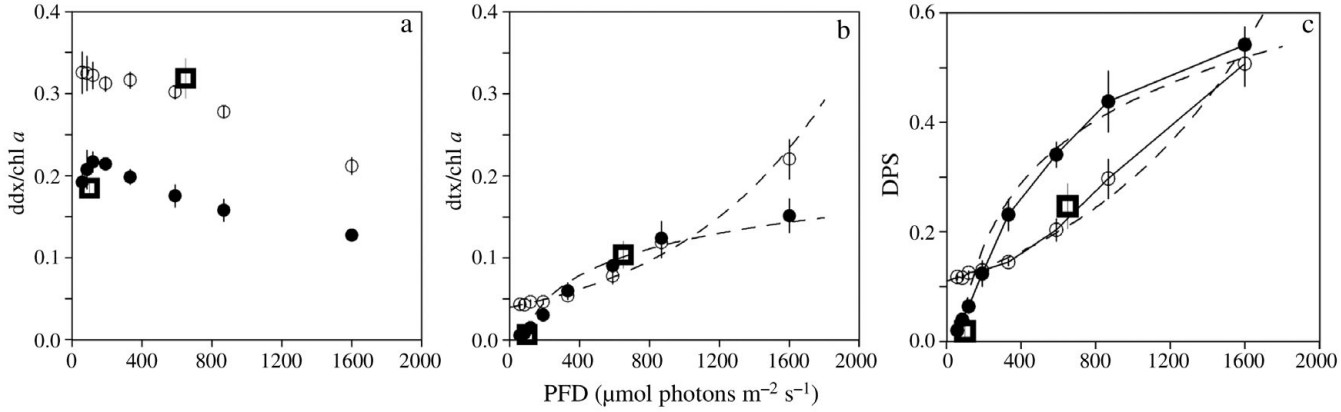

Fig. 6. *Symbiodinium*. Light dependence of the XC pigments (a) ddx:chl *a*, (b) dtx:chl *a* and (c) de-epoxidation state (DPS) for Strains A1-HL (○) and A1-LL (●) measured after 2 h exposure to different PFDs (light-response experiments), and at t_0 (data plotted versus growth PFD, □). Data are mean ± SE (n = 3). Details on the fits are in Table 3

and consequently RR and NPiR. Both Strains A1 and A1.1 appear to photoacclimate to the same extent when cultures are gradually shifted to HL (Hennige et al. 2009); thus the response by Strain A1, which demonstrates that growth under higher PFDs enables lower gross photoinhibition rates and less 'need' for repair, may also apply for Strain A1.1.

Data from the light-response curves provided further evidence for the mechanisms that reduce the susceptibility to damage in HL- versus LL-grown cells. RCII remained more oxidised (higher q_P) across all PFDs in HL- than LL-acclimated cells of Strain A1. Thus, the proportion of excitation energy used for photochemistry was markedly higher for HL-grown cells. This likely conferred a degree of photoprotection, since reduced RCIIs appear to be more susceptible to photodamage than oxidised RCIIs (Melis 1999). LL-grown cells exhibited a light-dependent decrease in q_P, i.e. a downregulation of photochemistry under high PFD, which would ultimately build up greater excitation pressure on PSII, leading to photoinhibition. In contrast, the NPQ achieved by the HL culture was lower or similar to that of the LL cells, probably due to the lower excitation pressure on RCII, i.e. a lower need for light dissipation. The described patterns of q_P and NPQ were clearly reflected in the 2-fold difference in the electron transport rates achieved by the 2 cultures, suggesting that HL cells had a greater photosynthetic capacity and hence a greater sink for photons compared to LL cells.

Pigment composition and PSII antenna size

The pigment composition of the light-harvesting antenna was markedly different for HL- as opposed to LL-grown cultures, but was quite similar for the 2 strains grown in LL (see Table 5 in Hennige et al. 2009). Pigment data from the light-response experiments revealed that HL-grown cells were more efficient in increasing the ratio of ΣPPC:ΣPSP during short-term (2 h) exposure to high PFD, with the effect of reducing the excitation energy transfer to the reaction centres, or perhaps acting as an antioxidant (Baroli et al. 2003). This was particularly evident in dnx, whose concentration increased for HL cells while remaining constant for LL cells. The extent of the light-driven increase of dnx suggests a photoprotective role for this pigment, either directly (e.g. antioxidant function) or indirectly as a precursor in the biosynthesis of other pigments (Swift et al. 1980).

XC pigment data demonstrated that *Symbiodinium* achieved similar DPS values under the highest PFD applied irrespective of the photoacclimation state. However, the light-response curves of XC concentrations revealed different extents of light activation of the light-dissipating mechanism in cells acclimated to different PFDs. Specifically, LL-grown cells maximised the XC at low-to-medium PFDs while HL-grown cells became more efficient at higher PFDs. This pattern paralleled that observed for the NPQ, confirming that the XC is indeed a primary pathway of dissipating excess excitation energy in the *Symbiodinium* tested (Gorbunov et al. 2001).

In spite of the light-driven increase in the ΣPPC:ΣPSP ratio in HL-grown cells, we did not observe any corresponding decrease in the PSII antenna size. In contrast, LL-grown cells exhibited an increase in σ_{PSII} after being exposed to PFD > 200 µmol photons m^{-2} s^{-1}, with the phenomenon being exacerbated in cultures treated with lincomycin. Curiously, this response is opposite to what would be expected as a result of photoacclimation to high PFD (i.e. a decrease in σ_{PSII}). In fact, increasing σ_{PSII} is likely to increase the susceptibility of

the RCIIs to damage (Vassiliev et al. 1994). In addition, the inverse linearity between changes in σ_{PSII} and F_v/F_m suggests that photoinactivated/photodamaged RCIIs continue transferring energy to the functional RCIIs; i.e. the RCIIs are well 'connected', with the effect of increasing the effective size of PSII antenna during photoinhibition, thus further exacerbating the effects of photoinhibition. Thus, the short-term (2 h) response of σ_{PSII} to supraoptimal light cannot be interpreted as a strategy of response to HL, but rather as a consequence. Such a pattern is in agreement with previous observations for the haptophyte *Emiliania huxleyi* (Ragni et al. 2008) and again explains the high values of σ_{PSII} observed in lincomycin-treated samples, where the inhibition of repair of photoinhibited RCII was considered the cause of the larger increase of the antenna size. This link between σ_{PSII} and photoinhibition is consistent with a 'lake' model for the organisation of the light-harvesting complex (Breton et al. 1979) in *Symbiodinium* with substantial overlap of the light-harvesting antennae of a population of RCIIs.

Our data for σ_{PSII} also demonstrate that the acclimation of *Symbiodinium* to HL does not involve a decrease in the size of its PSII antenna. This is consistent with the observations of Hennige et al. (2009) that different *Symbiodinium* genotypes, including Strain A1, grown under the same conditions as in the present study, preferentially modified their RC content when grown under LL versus HL, while keeping σ_{PSII} unvaried. Our study thus confirms that the predominant photoacclimation strategy in *Symbiodinium* involves changes in the cellular content of reaction centres (an 'n' strategy), in contrast to the 'σ' strategy that implies changes in the PSII antenna size (Iglesias-Prieto & Trench 1994).

Interspecific and phenotypic variability

Our study focused on the relative responses of 2 *Symbiodinium* phylotypes *ex hospite* (freely in suspension) and supports previous work demonstrating different photophysiological responses amongst different isolates of the same species (Suggett et al. 2007, 2009, Six et al. 2008), including *Symbiodinium* sp. (e.g. Robison & Warner 2006, Suggett et al. 2008, Hennige et al. 2009). Such differences reflect alternative adaptive strategies that enable species to exist across a range of environmental growth conditions; therefore, further work is warranted to determine whether the same patterns we observed here exist across the wider range of *Symbiodinium* phylotypes that predominate in nature.

A basic premise of our research was that differences in the susceptibility to photodamage and ability to repair photodamage between types resulted in different costs to their hosts, including corals, and ultimately in differences in their susceptibility to stress (e.g. Smith et al. 2005). However, because differences in the susceptibility of *Symbiodinium* to light stress have been reported between *in hospite* and *ex hospite* conditions (Bhagooli & Hidaka 2003, Buxton et al. 2009), further work is required to determine whether these same patterns are observed when *Symbiodinium* sp. growth is further modified *in hospite* of their cnidarian hosts, in particular where specific host–*Symbiodinium* associations exist. Although Bhagooli & Hidaka (2003) demonstrated that isolated zooxanthellae appear to be more susceptible to light stress when compared with the response *in hospite*, they did not eliminate the possibility that the light environment rather than the physiological susceptibility to stress was the key factor explaining the variability between *in-* and *ex hospite* conditions. Specifically, shading/light focusing by or within the host may have altered the light intensity to which the zooxanthaellae were exposed in the 2 conditions (e.g. Enriquez et al. 2005). The finding of Buxton et al. (2009), that *Symbiodinium* populations *in-* and *ex hospite* exhibited different physiological responses to inorganic carbon concentration and heat stress, actually was derived from the comparison of a *Symbiodinium* phylotype (*in hospite* of a coral) with those from an isolate (*ex hospite*) from different coral species. Therefore, the result is inconclusive because the same phylotype that has been isolated from different hosts is known to exhibit very different physiologies (see Hennige et al. 2009).

CONCLUSIONS

The 2 *Symbiodinium* phylotypes examined here possess several mechanisms to prevent HL-induced photoinhibition on relatively short time scales (hours). These span from antenna pigment changes (which may have antioxidant functions), to XC (NPQ) and PSII repair. Our study demonstrates that enhanced capacity to repair damaged RCIIs is the major mechanism conveying tolerance to acute HL exposure, i.e. conditions that are known to exacerbate the sensitivity of PSII activity to thermal stress and ultimately the sensitivity of host corals to bleaching. It remains to be tested if such a strategy is maintained by these algae when living inside the cnidarian host; if so, such mechanisms might provide an explanation for an algal system that has evolved to maximise light absorption (Enriquez et al. 2005) while still maintaining the capacity to regulate reaction centre damage. Such a strategy would be highly beneficial to both the alga and host in symbiosis. Importantly, photoacclimation can also play a significant role in minimising the need for photorepair by

reducing the potential excess of excitation energy upon PSII and so maintaining high photosynthetic rates. This would in turn result in high rates of ATP synthesis, thus additionally providing a greater potential for photorepair. The capacity to both photoacclimate and maintain photochemical (RCII) activity under high excitation pressure together appear to be key properties that determine the ultimate resistance of *Symbiodinium* genotypes to environmental stress.

Acknowledgements. This research was supported in part by the UK Natural Environment Research Council's (NERC) Surface Ocean Lower Atmosphere Study (SOLAS) directed programme through grant NE/C517168/1. S.J.H. was supported by a NERC PhD studentship. M.E.W. was supported by funding by the National Science Foundation (IOB 544765). We thank Dr. David Smith for helpful discussions and Dr. Phil Davey for technical support.

LITERATURE CITED

Adir N, Zer H, Shochat S, Ohad I (2003) Photoinhibition — a historical perspective. Photosynth Res 76:343–370

Arsalane W, Rousseau B, Duval JC (1994) Influence on the pool size of the xanthophyll cycle of the effects of light stress in a diatom: competition between photoprotection and photoinhibition. Photochem Photobiol 60:237–243

Baker NR, Oxborough K (2004) Chlorophyll *a* fluorescence as a probe of photosynthetic productivity. In: Papageorgiou GC, Govindjee (eds) Chlorophyll fluorescence. A signature of photosynthesis. Advances in photosynthesis and respiration, Vol 19. Springer, Dordrecht, p 65–82

Barlow RG, Cummings DG, Gibb SW (1997) Improved resolution of mono- and divinyl chlorophylls *a* and *b* and zeaxanthin and lutein in phytoplankton extracts using reverse phase C-8 HPLC. Mar Ecol Prog Ser 161:303–307

Baroli I, Do AD, Yamane T, Niyogi KK (2003) Zeaxanthin accumulation in the absence of a functional xanthophyll cycle protects *Chlamydomonas reinhardtii* from photooxidative stress. Plant Cell 15:992–1008

Behrenfeld MJ, Prasil O, Kolber ZS, Babin M, Falkowski PG (1998) Compensatory changes in Photosystem II electron turnover rates protect photosynthesis from photoinhibition. Photosynth Res 58:259–268

Bhagooli R, Hidaka M (2003) Comparison of stress susceptibility of *in hospite* and isolated zooxanthellae among five coral species. J Exp Mar Biol Ecol 291:181–197

Bilger W, Björkman O (1990) Role of the xanthophyll cycle in photoprotection elucidated by measurements of light-induced absorbance changes, fluorescence and photosynthesis in leaves of *Hedera canariensis.* Photosynth Res 25:173–185

Bouchard JN, Campbell DA, Roy S (2005) Effects of UV-B radiation on the D1 protein repair cycle of natural phytoplankton communities from three latitudes (Canada, Brazil, and Argentina). J Phycol 41:273–286

Breton J, Geacintov NE, Swenberg CE (1979) Quenching of fluorescence by triplet excited states in chloroplasts. Biochim Biophys Acta 548:616–635

Brown BE, Ambarsari I, Warner ME, Fitt WK, Dunne RP, Gibb SW, Cummings DG (1999) Diurnal changes in photochemical efficiency and xanthophyll concentrations in shallow water reef corals: evidence for photoinhibition and photoprotection. Coral Reefs 18:99–105

Buxton L, Badger M, Ralph P (2009) Effects of moderate heat stress and dissolved inorganic carbon concentration on photosynthesis and respiration of *Symbiodinium* sp. (Dinophyceae) in culture and in symbiosis. J Phycol 45: 357–365

Enriquez S, Mendez ER, Iglesias-Prieto R (2005) Multiple scattering on corals enhances light absorption by symbiotic algae. Limnol Oceanogr 50:1025–1032

Falkowski PG, Dubinsky Z (1981) Light-shade adaptation of *Stylophora pistillata*, a hermatypic coral from the Gulf of Eilat. Nature 289:172–174

Gorbunov MY, Kolber ZS, Lesser MP, Falkowaski PG (2001) Photosynthesis and photoprotection in symbiotic corals. Limnol Oceanogr 46:75–85

Hennige S, Suggett DJ, Warner ME, McDougall KE, Smith DJ (2009) Photobiology of *Symbiodinium* revisited: bio-physical and bio-optical signatures. Coral Reefs 28:179–195

Iglesias-Prieto R, Trench RK (1994) Adaptation and acclimation to irradiance in symbiotic dinoflagellates. I. Response of the photosynthetic unit to changes in photon flux density. Mar Ecol Prog Ser 113:163–175

Iglesias-Prieto R, Beltran VH, LaJeunesse TC, Reyes-Bonilla H, Thome PE (2004) Different algal symbionts explain the vertical distribution of dominant reef corals in the eastern Pacific. Proc Biol Sci 271:1757–1763

LaJeunesse TC (2001) Investigating the biodiviersity, ecology, and phylogeny of endosymbiotic dinoflagellates in the genus *Symbiodinium* using the ITS region: in search of a 'species' level marker. J Phycol 37:866–880

Lesser MP, Farrell JH (2004) Exposure to solar radiation increases damage to both host tissues and algal symbionts of corals during thermal stress. Coral Reefs 23:367–377

Lesser MP, Cullen JJ, Neale PJ (1994) Carbon uptake in a marine diatom during acute exposure to ultraviolet B radiation: relative importance of damage and repair. J Phycol 30:183–192

Levy O, Achituv Y, Yacoby YZ, Dubinski Z, Stambler N (2006) Diel tuning of coral metabolism: physiological responses to light cues. J Exp Biol 209:273–283

McCabe Reynolds J, Bruns BU, Fitt WK, Schmidt GW (2008) Enhanced photoprotection pathways in symbiotic dinoflagellates of shallow-water corals and other cnidarians. Proc Natl Acad Sci USA 105:13674–13678

Melis A (1999) Photosystem II damage and repair cycle in chloroplasts: what modulates the rate of photodamage? Trends Plant Sci 4:130–135

Olaizola M, La Roche J, Kolber Z, Falkowski PG (1994) Non-photochemical fluorescence quenching and the diadinoxanthin cycle in a marine diatom. Photosynth Res 41: 357–370

Provasoli L, McLaughlin JJA, Droop MR (1957) The development of artificial media for marine algae. Arch Mikrobiol 25:392–428

Ragni M, Airs RL, Leonardos N, Geider R (2008) Photoinhibition of PSII in *Emiliania huxleyi* (Haptophyta) under high light stress: the roles of photoacclimation, photoprotection, and photorepair. J Phycol 44:670–683

Robison JD, Warner ME (2006) Differential impacts of photoacclimation and thermal stress on the photobiology of four different phylotypes of *Symbiodinium* (Pyrrhophyta). J Phycol 42:568–579

Salih A, Larkum A, Cox G, Kühlh M, Hoegh-Guldberg O (2000) Fluorescent pigments in corals are photoprotective. Nature 408:850–853

Six C, Finkel ZV, Rodriguez F, Marie D, Partensky F, Campbell DA (2008) Contrasting photoacclimation costs in eco-

types of the marine eukaryotic picoplankter *Ostreococcus*. Limnol Oceanogr 53:255–265

Six C, Sherrard R, Lionard M, Roy S, Campbell DA (2009) Photosystem II and pigment dynamics among ecotypes of the green alga *Ostreococcus*. Plant Physiol 151:379–390

Smith DJ, Suggett DJ, Baker NR (2005) Is photoinhibition of zooxanthellae the primary cause of thermal bleaching in corals? Glob Change Biol 11:1–11

Suggett DJ, MacIntyre HL, Geider RJ (2003) Evaluation of biophysical and optical determinations of light absorption by Photosystem II in phytoplankton. Limnol Oceanogr Methods 2:316–332

Suggett DJ, Moore CM, Maranon E, Omachi C, Varela RA, Aiken J, Holligan PM (2006) Photosynthetic electron turnover in the tropical and subtropical Atlantic Ocean. Deep-Sea Res II 53:1573–1592

Suggett DJ, Le Floc'h E, Harris GN, Leonardos N, Geider RJ (2007) Different strategies of photoacclimation by two strains of *Emiliania huxleyi* (Haptophyta). J Phycol 43: 1209–1222

Suggett DJ, Warner ME, Smith DJ, Davey P, Hennige S, Baker NR (2008) Photosynthesis and production of hydrogen peroxide by *Symbiodinium* (Pyrrhophyta) phylotypes with different thermal tolerances. J Phycol 44:948–956

Suggett DJ, Moore CM, Hickman AE, Geider RJ (2009) Interpretation of fast repetition rate (FRR) fluorescence: signatures of phytoplankton community structure versus physiological state. Mar Ecol Prog Ser 376:1–19

Swift IE, Milborrow BV, Jeffrey SW (1980) Formation of neoxanthin, diadinoxanthin and peridinin from [^{14}C]zeaxanthin by a cell-free system from *Amphidinium carterae*. Phytochemistry 21:2859–2864

Takahashi S, Murata N (2008) How do environmental stresses accelerate photoinhibition? Trends Plant Sci 13:178–182

Takahashi S, Nakamura T, Sakamizu M, van Woesik R, Yamasaki H (2004) Repair machinery of symbiotic photosynthesis as the primary target of heat stress for reef-building corals. Plant Cell Physiol 45:251–255

Takahashi S, Whitney S, Itoh S, Maruyama T, Badger M (2008) Heat stress causes inhibition of the *de novo* synthesis of antenna proteins and photobleaching in cultured *Symbiodinium*. Proc Natl Acad Sci USA 105: 4203–4208

Takahashi S, Spencer M, Whitneya SM, Badger MR (2009) Different thermal sensitivity of the repair of photodamaged photosynthetic machinery in cultured *Symbiodinium* species. Proc Natl Acad Sci USA 106:3237–3242

Tchernov D, Gorbunov MY, de Vargas C, Narayan Yadav S, Milligan AJ, Häggblom M, Falkowski PG (2004) Membrane lipids of symbiotic algae are diagnostic of sensitivity to thermal bleaching in corals. Proc Natl Acad Sci USA 101:13531–13535

Vassiliev IR, Prasil O, Wyman KD, Kolber ZS, Hanson KA Jr, Prentice JE, Falkowski PG (1994) Inhibition of PS II photochemistry by PAR and UV radiation in natural phytoplankton communities. Photosynth Res 42:51–64

Venn AA, Wilson MA, Trapido-Rosenthal G, Keely BJ, Douglas AE (2006) The impact of coral bleaching on the pigment profile of the symbiotic alga, *Symbiodinium*. Plant Cell Environ 29:2133–2142

Warner ME, Berry-Lowe S (2006) Differential xanthophylls cycling and photochemical activity in symbiotic dinoflagellates in multiple locations of three species of Caribbean coral. J Exp Mar Biol Ecol 339:86–95

Warner ME, Fitt WK, Schmidt GE (1999) Damage to Photosystem II in symbiotic dinoflagellates: a determinant of coral bleaching. Proc Natl Acad Sci USA 96:8007–8012

Warner ME, Chilcoat GC, McFarland FK, Fitt WK (2002) Seasonal fluctuations in the photosynthetic capacity of Photosystem II in symbiotic dinoflagellates in the Caribbean reef-building coral *Montastraea*. Mar Biol 141: 31–38

Yakovleva I, Hidaka M (2004) Differential recovery of PSII function and electron transport rate in symbiontic dinoflagellates as a possible determinant of bleaching susceptibility of corals. Mar Ecol Prog Ser 268:43–53

Editorial responsibility: Hans Heinrich Janssen, Oldendorf/Luhe, Germany

Submitted: April 22, 2009; Accepted: March 8, 2010
Proofs received from author(s): April 30, 2010